IMPACTS OF LARGE-SCALE SURFACE MODIFICATIONS ON METEOROLOGICAL CONDITIONS AND ENERGY USE: A 10-REGION MODELING STUDY

Haider Taha, Steven Konopacki, and Sasa Gabersek
Heat Island Project
Environmental Energy Technologies Division

FINDINGS

Several field-monitoring studies have shown that using high-albedo materials on and increasing vegetative fraction around buildings can save a significant amount of cooling energy use. Also, meteorological and photochemical modeling studies suggest that large-scale increases in albedo (e.g., of buildings and paved surfaces) and vegetative fraction can have beneficial impacts on urban climates and air quality. These earlier studies pointed to the need for a multi-regional assessment of the meteorological and energy-use impacts of surface modifications. They also pointed to the need for assessing these impacts on a year-round basis, e.g., quantifying potential penalties in heating energy use in winter in addition to savings in cooling energy use in summer. The study described in this paper is a first step in that direction.

This paper summarizes results from a mesoscale modeling study to quantify the possible meteorological and energy-use impacts of large-scale increases in surface albedo and vegetative fraction. Ten regions in the U.S. were characterized and simulated in base- and modified-surface conditions. Time- and space-dependent meteorological variables were simulated for each region in four 3-day episodes to represent a range of seasonal variations.

The base-case mesoscale simulations suggest heat islands of 1-2°C in most urban areas analyzed in this study. The simulations also suggest that large-scale increases in surface albedo and vegetative fraction can almost offset the urban heat island intensity in most of these areas. The energy implication of a 1-2°C reduction in space-averaged air temperatures (around 2 pm local time) is a decrease of up to 10% in peak electricity demand. In terms of annual costs of energy use, the simulations suggest net savings in the order of \$10-35 per 100 m^2 of roof area depending on building type and region. Areas like Los Angeles, Houston, Miami, and Phoenix seem to benefit most from the large-scale surface modifications described in this paper, whereas regions like Philadelphia seem to benefit the least.

Theor. Appl. Climatol. 00, 000–000 (1998)

Theoretical and Applied Climatology

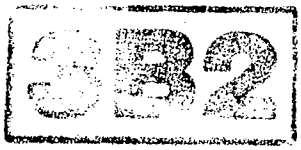

[1] Lawrence Berkeley National Laboratory, Berkeley, California, U.S.A.
[2] Heat Island Project, Environmental Energy Technologies Division, Lawrence Berkeley National Laboratory, Berkeley, California, U.S.A.

Impacts of Large-scale Surface Modifications on Meteorological Conditions and Energy use: A 10-Region Modeling Study

Haider Taha[1], Steven Konopacki[2], and Sasa Gabersek[2]

With 6 Figures

Received December 1, 1996
Revised May 11, 1998

Summary

This paper summarizes results from a mesoscale modeling study to quantify the possible meteorological and energy-use impacts of large-scale increases in surface albedo and vegetative fraction. Ten regions in the U.S. were characterized and simulated in base- and modified-surface conditions. Time- and space-dependent meteorological variables were simulated for each region in four 3-day episodes to represent a range of seasonal variations.

In terms of peak summer conditions, for example, the mesoscale simulations suggest that at 2 pm local time, urban areas in Los Angeles, New York, Chicago, Atlanta, Washington DC, and Philadelphia can be up to 2 °C warmer than their rural surrounds, whereas Dallas and Houston can be 1.5 °C and Phoenix up to 1 °C warmer than rural areas. Miami does not exhibit a significant heat island. The simulations also suggest that large-scale increases in albedo and vegetative fraction can result in spatially-averaged decreases in 2-pm air temperature of 0.5 to 1.5 °C during a typical summer day, depending on region.

Using a simple interpolative procedure, a complete year of hourly weather data was created for each region (based on episodic meteorological simulation results) and input into energy-use models. The modified weather input was used to assess the effects of large-scale albedo and vegetative fraction changes on annual energy consumption in each of the ten areas targeted in this study. The simulations suggest annual electricity savings of between 1 and 6.7 kWh m^{-2} (of roof area) in residential neighborhoods and between 2 and 6.1 kWh m^{-2} in office areas, depending on region. Annual gas penalties amount to up to 33 kBtu m^{-2} (of roof area) in residential neighborhoods and up to 20 kBtu m^{-2} in office areas.

1. Introduction

Several field-monitoring studies have shown that using high-albedo materials on and increasing vegetative fraction around buildings can save a significant amount of cooling energy use (e.g., Akbari, et al. 1997a, b; Simpson and Mcpherson, 1997; Parker and Barkaszi, 1997). Also, meteorological and photochemical modeling studies suggest that large-scale increases in albedo (e.g., of buildings and paved surfaces) and vegetative fraction can have beneficial impacts on urban climates and air quality (Taha et al., 1988; Taha, 1996, 1997). These field experiments and numerical modeling work suggest that energy savings on the order of 30% or larger are achievable and that improvements in ozone air quality on the order of 20% may be possible in summer. These earlier studies pointed to the need for a multi-regional assessment of the meteorological and energy-use impacts of surface modifications. They also pointed to the need for assessing these impacts on a year-round basis, e.g., quantifying potential penalties in heating energy use in winter in addition to savings in cooling energy use in summer. The study described in this paper is a first step in that direction.

The meteorological impacts of increased surface albedo and vegetative fraction were simu-

lated for ten regions in the U.S. (Southern California, Central Georgia, South and Central Texas, Eastern Pennsylvania, Connecticut, Downstate New York, District of Columbia, Maryland, Northern Virginia, Delaware, New Jersey, Southern Florida, and Central Arizona). These regions were selected to represent a variety of climate conditions and also because most of their urban areas are in non-attainment status for ozone.

Each region was simulated in four, three-day episodes using a modified version of the Colorado State University Mesoscale Model (CSUMM). For each episode, two scenarios were simulated: a base case to represent existing conditions and a modified case corresponding to increased albedo and vegetative fraction. For each region, gridded input to the meteorological model was developed based on land-use/land-cover and remote-sensed data. A simple interpolative method was devised to create a whole year of hourly weather for input in building energy simulation models (e.g., DOE-2) based on results from episodic mesoscale meteorological simulations.

2. Modeling Assumptions

This study uses a three-dimensional, Eulerian, mesoscale meteorological model (CSUMM) to simulate the base case and modified conditions in the areas of interest. The model was modified to use gridded surface characteristics input and to include a bulk-layer vegetation parameterization (Sailor, 1993). Taha (1996, 1997) describes the model, its input, initial, and boundary conditions. For information on model formulation, development, and assumptions, refer to Pielke (1974, 1984) and Kessler and Douglas (1992). At the end of this paper, a brief discussion of the model formulation and its evaluation for this application is also given.

Four 3-day meteorological episodes were simulated for each region, i.e., January 25–27, March 25–27, May 25–27, and July 25–27, to represent a range of seasonal conditions. For each region and episode, one base case and one modified scenario were simulated. The modeling domains are identified in Table 1.

2.1 Surface Characterization

The gridded surface characteristics input to the meteorological model was developed based on U.S. Geological Survey (USGS) data and, for the Los Angeles basin, also on satellite (AVHRR) and other data (Liu, 1994; Horie et al., 1990). Two types of USGS data were used to derive gridded surface characteristics. The first, the Digital Elevation Model (DEM) consists of gridded topography data. The second, Land Use and Land Cover (LULC) data, provides information on nine major classes of land use. The category of most interest to this modeling study (because of its potential for surface modification) is "urban" land use, which is further divided into seven sub-categories as shown in Table 2. For all urban LULC sub-categories, we assumed a soil moisture content (soil wetness) of 0.05, density of $1.6\,g\,cm^{-3}$, thermal diffusivity of $0.0033\,cm^2\,s^{-1}$, and specific heat of $1.26\,J\,g^{-1}\,K^{-1}$ (based on Pielke, 1984). Other, non-constant urban parameters are given in Table 2. The value for Q_f given in Table 2 is the maximum for the given LULC. This maximum is then scaled using a Fourier series to calculate hourly values of Q_f for each

Table 1. *Modeling Domains Simulated in this Study.* (Numbers in parenthesis refer to the UTM zone)

Region	UTM West Boundary	UTM East Boundary	UTM South Boundary	UTM North Boundary	Modeling domain Area	Land portion (%)
Atlanta GA (16)	592.5 km	957.5 km	3552.5 km	3872.5 km	116,800 km^2	99
Chicago IL (16)	337.5 km	662.5 km	4437.5 km	4762.5 km	105,625 km^2	80
Dallas TX (14)	502.5 km	867.5 km	3437.5 km	3757.5 km	116,800 km^2	98
Houston TX (14)	122.5 km	497.5 km	3107.5 km	3427.5 km	120,000 km^2	60
Los Angeles CA (11)	275.5 km	600.5 km	3670.5 km	3870.5 km	65,000 km^2	83
Miami FL(17)	302.5 km	697.5 km	2657.5 km	2987.5 km	130,350 km^2	20
New York NY (18)	417.5 km	747.5 km	4322.5 km	4647.5 km	107,250 km^2	60
Philadelphia PA (18)	322.5 km	667.5 km	4207.5 km	4537.5 km	110,550 km^2	55
Phoenix AZ(12)	227.5 km	587.5 km	3547.5 km	3867.5 km	115,200 km^2	99
Washington DC (18)	162.5 km	497.5 km	4102.5 km	4427.5 km	108,875 km^2	65

Table 2. *Some Thermophysical Properties Assumed for Urban LULCs. Based on Pielke (1984) and Gabersek and Taha (1996)*

Urban LULC	Modifiable	α^1	Z_o	Q_f	η^2
Residential	•	0.16	35	10.0	0.20
Commercial/Services	•	0.14	150	10.0	0.05
Industrial	•	0.20	35	10.0	0.05
Transp./Communic./Utilit.		0.16	35	40.0	0.05
Indust./Commercial Complexes	•	0.14	35	40.0	0.05
Mixed urban or built-up	•	0.16	35	10.0	0.05
Other urban/built-up		0.14	35	10.0	0.05

In this table, α is albedo, Z_o is roughness length (cm), Q_f is maximum anthropogenic heat flux ($W\,m^{-2}$) for corresponding LULC, and η is vegetative fraction.

[1] Used only where AVHRR-based albedo data was unavailable, e.g., regions other than the Los Angeles basin.

[2] Used only where vegetation biomass data was unavailable, e.g., regions other than the Los Angeles basin.

LULC. Table 3 shows values of parameters assigned to other, non-urban LULCs.

In this study, each mesoscale model grid cell of area A (5×5 km), is subdivided into ~625 subregions, each ~200 m×200 m (original USGS LULC grid cells). The average value of a parameter P in area A is then calculated through algebraic averaging:

$$P = \frac{1}{A}\Sigma P_i A_i \tag{1}$$

where P_i is the value of a parameter in sub-area A_i. This method was used for all parameters except roughness length which was computed from the logarithmic wind profile equation:

$$u(z) = \frac{u^*}{k} \ln\left(\frac{z - z_d}{Z_o}\right) \tag{2}$$

where u^* is friction velocity, k is von Karman constant, z is height, z_d is displacement height and Z_o is roughness length. Assuming $u = 1/A\,\Sigma u_i A_i$, and averaging yields:

$$Z_o = \prod_i Z_{oi}^{A_i/A} \tag{3}$$

where Z_{oi} is the roughness length of LULC (i) whose area is A_i. An approach similar to that in equation (3) has been used by other researchers as well (e.g., Vihma and Savijarvi, 1991).

The averaging depicted by Eq. (1) and (3) is reasonable in the context of this study since the mesoscale model does not explicitly treat sub-grid-scale variability in surface properties or meteorological conditions. Explicit treatment of canopy-layer dynamics is not yet a feasible feature in mesoscale models, and sub-grid-scale variability in surface properties can be accounted for only through this type of averaging.

In addition to establishing base-case surface characteristics, gridded input for a modified-surface scenario for each region was also developed. The modified scenario presented in this paper corresponds to simultaneously increasing albedo and vegetative fraction according to:

$$\alpha'_{ij} = \alpha_{ij} + \delta\alpha \sum_{L=1}^{n} f_{\alpha L_{ij}} \tag{4}$$

$$\eta'_{ij} = \eta_{ij} + \delta\eta \sum_{L=1}^{n} f_{\eta L_{ij}} \tag{5}$$

where α' and α are new and basecase albedos for cell (i, j), respectively, $\Delta\alpha$ is a nominal increase in albedo, f_α is the area fraction of modifiable land use "L" in cell (i, j), η' and η are the new and basecase vegetative fractions in cell (i, j) respectively, $\delta\eta$ is a nominal increase in vegetative fraction, and f_η is the area fraction of modifiable land use "L" in cell (i, j). The land uses that are assumed modifiable (i.e., to which the fractions "f" are applied) are the ones marked in the "Modifiable" column in Table 2. None of the categories listed in Table 3 are subject to modification.

The nominal albedo increase for the modified scenario was $\delta\alpha = +0.15$ and that for vegetative fraction was $\delta\eta = +0.15$. This scenario translates into a space-averaged albedo increase of 0.03–0.05 and a space-averaged vegetative fraction increase of 0.03–0.04, i.e., averaged over the number of modified cells.

Table 3. *Thermophysical Properties Assumed for non-Urban LULCs*

Non-urban LULC	α	Z_o	s	ρ	k	c	Q_f	η
Cropland/pasture	0.18	12	0.30	1.8	0.0038	0.44	0.0	0.60
Orchards/groves	0.16	12	0.30	1.8	0.0038	0.44	0.0	0.60
Confined feeding	0.12	12	0.30	1.8	0.0038	0.44	0.0	0.60
Agricultural	0.15	12	0.30	1.8	0.0038	0.44	0.0	0.60
Herbaceous rangeland	0.18	5	0.03	1.6	0.0050	0.30	0.0	0.10
Shrub/brush rangeland	0.18	5	0.03	1.6	0.0050	0.30	0.0	0.10
Mixed rangeland	0.18	5	0.03	1.6	0.0050	0.30	0.0	0.10
Deciduous forest	0.15	350	0.20	1.8	0.0057	0.35	0.0	0.50
Evergreen forest	0.18	350	0.20	1.8	0.0057	0.35	0.0	0.50
Mixed forest	0.16	350	0.20	1.8	0.0057	0.35	0.0	0.50
Streams/canals	0.08	1	1.00	1.0	0.0015	1.00	0.0	0.0
Lakes	0.06	1	1.00	1.0	0.0015	1.00	0.0	0.0
Reservoirs	0.08	1	1.00	1.0	0.0015	1.00	0.0	0.0
Bays/estuaries	0.06	1	1.00	1.0	0.0015	1.00	0.0	0.0
Forested wetland	0.16	0.001	0.50	1.5	0.0020	0.80	0.0	0.25
Nonforest wetland	0.16	0.001	0.50	1.5	0.0020	0.80	0.0	0.25
Dry salt flats	0.40	0.05	0.01	1.6	0.0050	0.30	0.0	0.0
Beaches	0.40	0.05	0.01	1.6	0.0050	0.30	0.0	0.0
Sandy/non beach	0.30	0.05	0.01	1.6	0.0050	0.30	0.0	0.0
Bare rock	0.30	0.05	0.01	1.6	0.0050	0.30	0.0	0.0
Mines/quarries/pits	0.25	0.05	0.01	1.6	0.0050	0.30	0.0	0.0
Transitional areas	0.18	0.05	0.01	1.6	0.0050	0.30	0.0	0.0
Mixed barren land	0.18	0.05	0.01	1.6	0.0050	0.30	0.0	0.0
Shrub/brush tundra	0.18	10	0.05	1.3	0.0038	0.35	0.0	0.20
Herbaceous tundra	0.18	10	0.05	1.3	0.0038	0.35	0.0	0.20
Bare ground	0.16	10	0.05	1.3	0.0038	0.35	0.0	0.20
Wet tundra	0.20	10	0.05	1.3	0.0038	0.35	0.0	0.20
Mixed tundra	0.19	10	0.05	1.3	0.0038	0.35	0.0	0.20
Perennial snow	0.80	0.005	0.20	0.8	0.0100	0.21	0.0	0.0
Glaciers	0.35	0.005	0.20	0.8	0.0100	0.21	0.0	0.0

In this table, α is albedo, Z_o is roughness length (cm), s is surface wetness, ρ is density (g cm^{-3}), k is thermal diffusivity (cm^2 s^{-1}), c is specific heat (J g^{-1} K^{-1}), Q_f is maximum anthropogenic heat flux (W m^{-2}) for corresponding LULC, and η is vegetative fraction. Data after Pielke (1984) and Gabersek and Taha (1996).

A discussion of potential, inadvertent impacts of increased albedo is in order. In residential areas, where the bulk of the albedo increase will tend to occur, most buildings are 1–3 stories high and are mostly uniform in height. Thus the increased reflected portion of incident solar radiation will likely not be absorbed by surrounding structures. This latter situation could arise, however, when a mix exists of low and tall structures so that increasing the albedo of roofs on lower structures would tend to increase the reflected radiation absorbed at the walls of the taller ones. But this kind of mix is usually very limited in extent, e.g., downtown areas where highrise buildings are immediately surrounded by much lower structures. Thus, except for these limited instances, it is expected that the increase in a average albedo (in each grid cell) is directly proportional to the area-weighted increase in albedo of the building and paving materials.

Another factor to consider is that albedo depends on solar angle and can thus vary during the course of the day. The albedo specified in Eq. (4) is a daytime-averaged albedo and the amount of increase is added to that daytime average value. But in fact, the diurnal change in albedo may not be as large as this discussion seems to suggest, especially when integrated over a grid

cell which is 5×5 km in area. For example, the work of Sievers and Zdunkowski (1985) and Aida (1982) suggests that urban albedo can change by at most 10% during the very early sunrise or sunset hours. During most of the daytime, however, the change in albedo, due to changing solar angle, is less than 5%. Thus the assumption that, on a grid cell of 5×5 km, the fluctuation in effective albedo over daytime hours is small, is a reasonable one and, thus, Eq. (4) is justifiable.

2.2 Initial Conditions

Data needed to initialize the seasonal episodic meteorological simulations were based on observations. A representative sounding station within each of the ten modeling domains was selected and 1200Z-profiles were obtained including pressure, temperature, dew-point depression, wind direction, and wind speed from the surface to the 100-mb pressure level. These variables were used to derive others, e.g., specific humidity, required by the model. Figures 1 and 2 show example initial conditions for Dallas TX and Washington DC, respectively.

2.3 Energy-Use Modeling

In addition to modeling the meteorological effects of changes in albedo and vegetative fraction as described above, the energy impacts of meteorological changes were simulated with the DOE-2 model (BESG 1990). DOE-2 is a state-of-the-science building energy simulation tool that calculates annual air-conditioning and heating energy use on an hourly basis given building prototypes and climatic data. As input, DOE-2 takes hourly weather data for an entire year as well as a complete and detailed description of the building, its site, operation schedules, internal loads, shell, and heating, ventilating, and air-conditioning systems.

In DOE-2 simulations, albedo was increased from 0.25 to 0.55 on residential roofs and from 0.25 to 0.70 on office roofs. These changes are based on the levels of albedo increase demonstrated in the field, e.g., by Akbari et al. (1997a). On the other hand, the vegetation increase was modeled in DOE-2 as an additional three trees per residential or commercial unit. The trees were "placed" on the south side of a building and each was modeled as a cube 7.5 m on the side, with a solar radiation transmissivity of 0.1 in summer and 0.9 in winter. Four prototypical buildings were simulated with DOE-2: one old and one new residential and one old and one new office buildings. In this study, it is assumed that cooling is done with electricity and heating with gas. For a description and discussion of the development of these prototypes, refer to Konopacki et al. (1997).

2.4 Creating Hourly Modified Weather

Because the CSUMM, as any other mesoscale model, is typically run for episodes of two to five days at a time while the DOE-2 model is

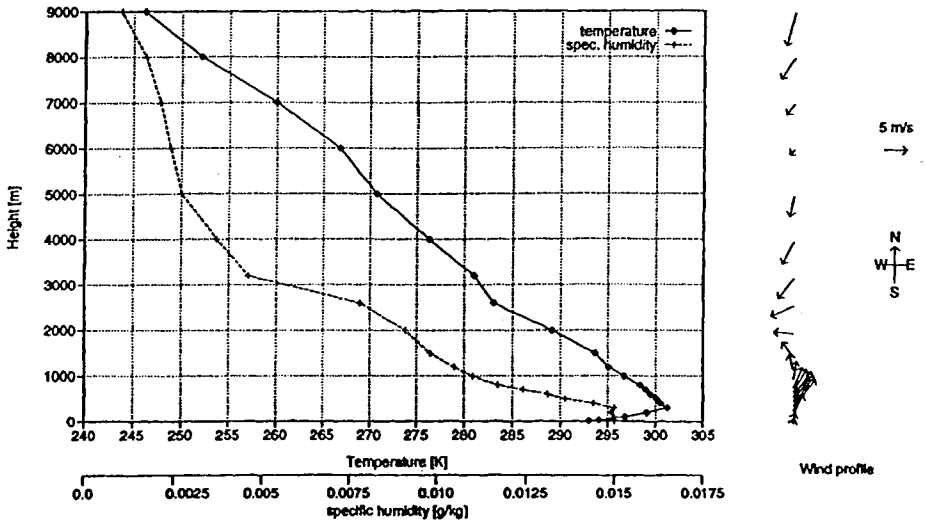

Fig. 1. Initial conditions (observational data) for the Dallas TX modeling domain at 1200Z on July 25. Wind is displayed in top-view fashion, i.e., u-v vector at the corresponding heights

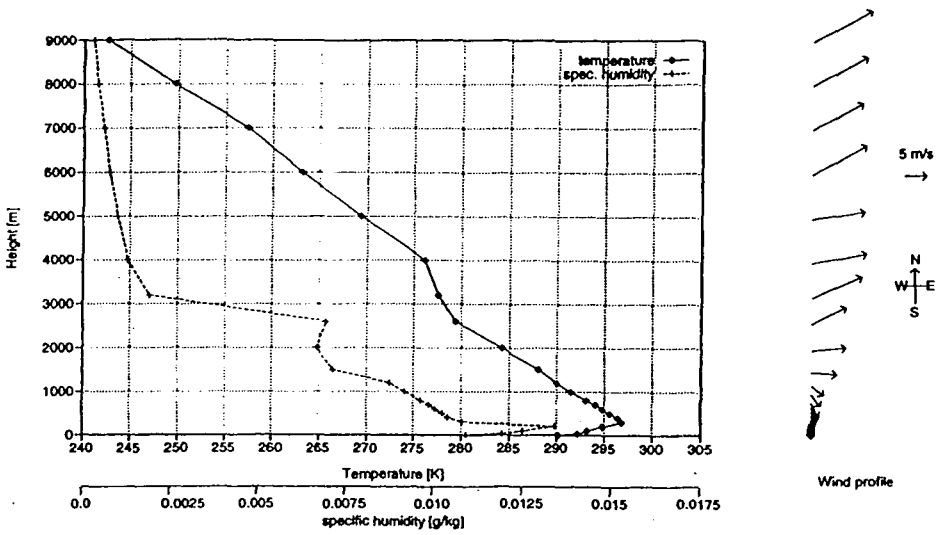

Fig. 2. Initial conditions (observational data) for the Washington DC modeling domain at 1200Z on July 25

typically run on an hourly basis for a whole year, the issue was to create a complete year of hourly modified weather data (for DOE-2 input) based on multi-episodic simulation results from CSUMM. A simple interpolative procedure was devised to modify an original Typical Meteorological Year (TMY) weather file for each region based on the differences between averaged simulated base and modified meteorological conditions (i.e., as simulated by CSUMM). In this preliminary approach, only air temperature was modified. This, as mentioned earlier, is because the impacts of modifications in surface properties on the wind and atmospheric moisture fields are negligible compared to the impacts on air temperature, as suggested by the mesoscale simulations to date.

In this simple interpolative procedure, a TMY file (i.e., base-case weather) for a region of interest is read on an hourly basis. As a first filter, air temperature during those hours with cloud cover greater than 7 tenths, or alternatively, those with rain or snow, is not modified. For the remaining hours, the decrease in air temperature is calculated based on a linear regression between air temperature depression and absolute air temperature simulated by the mesoscale model. Seasonal regression correlations for each region are developed based on multi-episodic meteorological simulations. These different correlations are applied to different parts of the year in the TMY weather record. In addition, and while performing this calculation, it is also assumed that there exists a time lag of 2 hours. This means, for instance, that the effects of surface modification on air temperature will not be detected before two hours have lapsed following onset of sunshine, e.g., two hours after an overcast period or two hours after sunrise on a clear day, and that temperature depression extends through two hours after sunset on a clear and warm day. The cloud cover threshold (7/10) and time lag (2 hours) are arbitrary but reasonable. Further enhancement to this interpolation method is planned for the future.

3. Results

For peak summer conditions, the mesoscale simulations of the 10 regions suggest that most urban areas are heat islands of about 1–2 °C. For example, at 2pm on a late-July or early-August day, urban areas in Los Angeles, Atlanta, Chicago, New York, Philadelphia, and Washington DC can be ~2 °C warmer than their rural surrounds. A heat island of about 1.5 °C is simulated in Dallas and Houston and 1 °C in Phoenix. Urban Miami has a negligible heat island (less than 0.5 °C). As an example, Figs. 3 and 4 show the simulated temperature field at 2pm on July 26 in the central Texas and Washington DC modeling domains. Urbanized areas, e.g., Dallas and Fort Worth, appear to be 1–1.5 °C warmer than their surroundings whereas the Washington

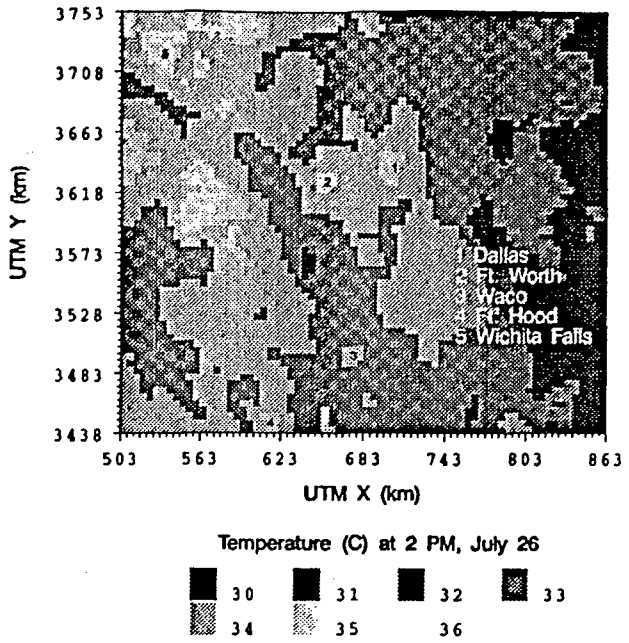

Fig. 3. Simulated air temperature (lowest atmospheric layer) at 2pm, July 26, for the central Texas modeling domain. Dallas and Fort Worth are at 35.5 °C, their immediate surrounds at 34 °C, and the distant surrounds at 33 °C. Other urbanized areas are about 1 °C warmer than their surrounds, e.g., Fort Hood, Waco, and Wichita Falls

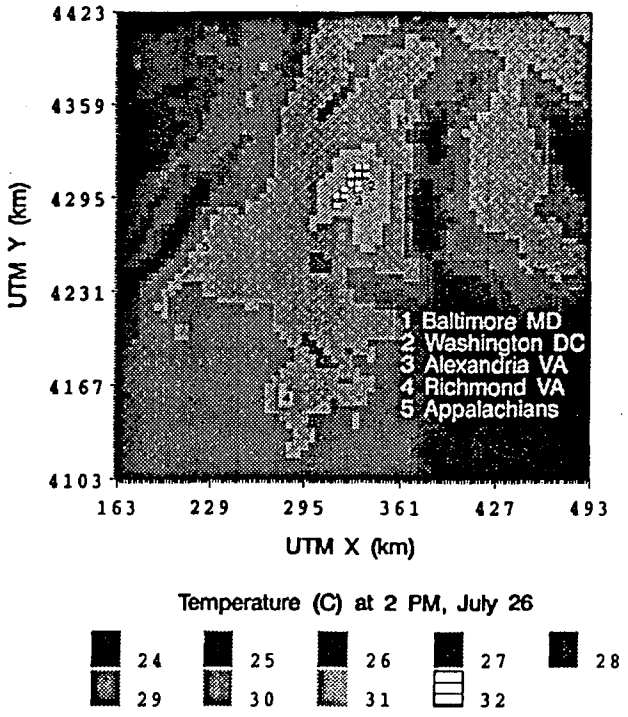

Fig. 4. Simulated air temperature (lowest atmospheric layer) at 2pm, July 26, for the District of Columbia modeling domain. The Washington-Alexandria cluster is at 32.2 °C whereas the immediate surrounds are at 31 °C, and the distant surrounds at 30 °C. Both Baltimore MD and Richmond VA are about 1 °C warmer than their surrounds

Table 4. *Simulated Heat Islands (rounded to nearesat 0.5 °C) and Corresponding Increases in Peak Electricity Demand*

Region	Simulated ΔT (urban)-(rural)	Slope of peak demand (%/°C)**	Percent increase in peak due to ΔT
Los Angeles	2	2.7	5.4
Chicago	2	2.7	5.4
Atlanta	2	5.4	10.8
Washington DC	2	2.7	5.4
Philadelphia	2	1.4	2.8
New York	2	2.7	5.4
Houston	1.5	5.4	8.1
Dallas	1.5	5.4	8.1
Phoenix	1	5.4	5.4
Miami	~0	5.4	~0

** Slope factors based on Linder and Inglis (1989).

DC – Alexandria VA cluster appears to be ~1 °C warmer than its immediate surrounds but ~2 °C warmer than the more distant surrounds.

Table 4 lists the simulated peak-hour summer heat island for ten cities (rounded to the nearest 0.5 °C). And, to give an idea as to the possible impacts of these heat islands on electricity demand, the corresponding estimated percent increases in regional peak demand are given. These suggest that between 3 and 10% of the peak demand (around 2 pm) may be caused by the higher urban air temperatures. Areas like Atlanta, Houston, and Dallas seem to be the most impacted, whereas Philadelphia and Miami the least so.

The changes in surface properties (i.e., increased albedo and vegetative fraction) can affect all meteorological variables. However, according to sensitivity simulations in this study, the most significant changes occur in the temperature field. In terms of changes in the wind field, the surface modifications discussed in this paper have a relatively negligible impact. In locations where a land-sea breeze circulation exists, the increased land albedo or vegetative cover tend to weaken the sea-breeze slightly, e.g., by a change of less than 1 ms^{-1}. In inland regions, i.e., not affected by a major water body, the changes in surface properties cause a similar small change in the wind field as the pressure gradient between urban and non-urban areas changes slightly following surface modification.

Table 5. *Spatially-averaged Simulated Temperature Decrease (Rounded to the Nearest 0.5 °C) and Coincident Absolute Temperature for ten Regions*

Region	$\langle\Delta T\rangle$ $(°C)^{max}$	$\langle T\rangle$ $(°C)^{max}$
Los Angeles CA	−1.5	33.2
Chicago IL	−1.0	29.0
Atlanta GA	−1.0	31.0
Washington DC	−0.5	31.2
Philadelphia PA	−1.0	31.0
New York NY	−1.0	26.0
Houston TX	−1.0	32.9
Dallas TX	−1.0	33.0
Phoenix AZ	−1.0	37.0
Miami FL	−0.5	28.5

In terms of air temperature, the meteorological simulations suggest that increased surface albedo and vegetative fraction, as defined in Eq. (4) and (5), can result in cooling of up to 5 °C locally, i.e., at one particular 5×5-km grid cell. But the gridded air temperature depression field simulated by CSUMM was averaged to obtain a more representative (weighted) regional temperature decrease and, thus, a more realistic modified weather input to energy simulations for each region. Another reason for computing a spatially-averaged temperature depression is to limit the energy simulations to one weather input per region (which is the norm in DOE-2 modeling). This temperature averaging was done over grid cells where surface modifications were assumed.

Table 5 is a "snapshot" summary of the simulated temperature impacts of the modified scenario described earlier. This snapshot is for peak hour (~2 pm) on a clear summer day showing the spatially-averaged decrease in temperature and the spatially-averaged coincident absolute air temperature. One factor determining the possible decrease in temperature is the extent of modification, that is, the area affected by increased albedo and vegetative fraction. The larger the modified area, the larger $\langle\Delta T\rangle$. Thus, the largest change in air temperature is seen in the Los Angeles basin.

On the other hand, the year-round, spatially-averaged decreases in air temperature were calculated using the interpolation procedure mentioned earlier. For example, Figs. 5 and 6 show hourly temperature differences (for a whole year) for the Dallas/Ft. Worth and Washington DC areas, respectively. The figures show the difference between original (TMY) and modified-temperature input to the DOE-2 model based on the space-averaged mesoscale temperature simulation results of these regions. Although each hourly temperature reduction of the year is shown, these figures are intended to give only a qualitative impression of the impacts of the modified scenario on a year-round basis. Aspects to note include 1) the temperature reduction is generally larger in the Dallas region than in the Washington DC region, 2) the reduction in each region is larger in summer than in winter, and 3) that there is essentially no reduction in temperature in fall and winter in the Washington DC area

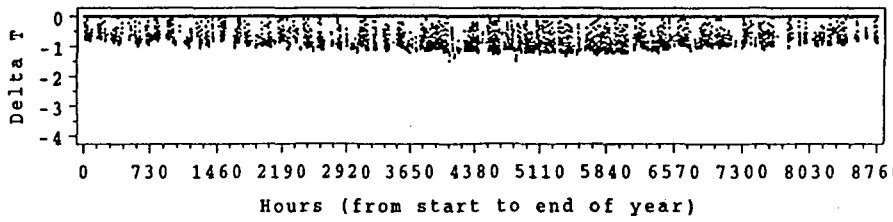

Fig. 5. Space-averaged simulated air temperature difference (modified scenario minus basecase) for 8760 hours (one year) in the Dallas – Ft. Worth TX area

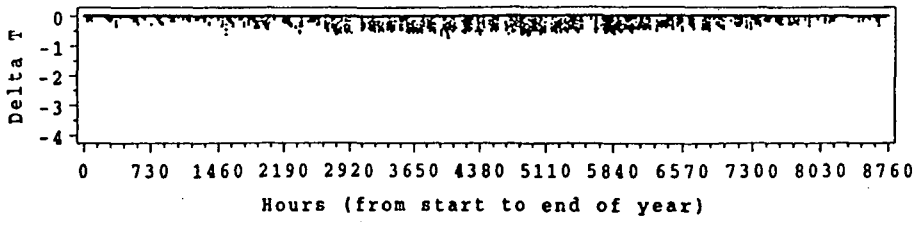

Fig. 6. Space-averaged simulated air temperature difference (modified scenario minus basecase) for 8760 hours (one year) in the Washington DC area

Table 6. *Averaged Energy Savings, Penalties, and Costs of Large-scale Increases in Albedo and Vegetative Fraction*

	Peak electricity savings (W/100 m^2 of roof area)		Annual electricity savings (kWh/100 m^2 of roof area)		Annual gas penalties (kBtu/100 m^2 of roof area)		Annual cost savings ($/100 m^2 of roof area)**	
	Res.	Office	Res.	Office	Res.	Office	Res.	Office
Atlanta	202	304	287	332	925	725	17	21
Chicago	208	257	192	222	2189	1480	10	11
Los Angeles	412	472	432	610	869	306	37	52
Ft. Worth	305	276	408	425	774	613	27	25
Houston	299	362	420	413	535	317	36	30
Miami	195	172	465	431	15	0	37	30
New York	296	217	168	209	1797	1164	12	19
Philadelphia	237	215	105	230	3336	2021	−9	15
Phoenix	276	215	679	613	202	184	71	55
Washington DC	218	247	256	266	1328	1021	8	13

** These are net dollar savings, that is, they include the penalties in heating gas as well as the savings in cooling electricity.

(since the synoptic conditions do not favor temperature reduction as a result of increased surface albedo and vegetative fraction, i.e., overcast conditions, snow, and rain).

To assess the annual energy use impacts of the modified scenario, original and modified weather input was used in DOE-2 simulation of four prototypical buildings. Although the same prototypes were used in all regions, their heating/cooling system-component sizes were region-specific (Konopacki et al., 1997). The costs of electricity and gas are also region-dependent. Table 6 summarizes the DOE-2 simulation results in a condensed manner. The simulations were performed separately for old and newer building types, but in Table 6 these are averaged to give one single number per case per city. It is important to note that these results are for total effects (i.e., building envelope effect plus air temperature effect of increased albedo and vegetation).

The only apparent anomaly is that of annual costs savings in residential buildings in Philadelphia, which shows a penalty of $9 per 100 m^2 roof-area per year. This is due to the combined effects of larger needs for winter heating than summer cooling and somewhat higher gas prices in the Philadelphia area. Cost-wise, the best results are seen in Phoenix, Los Angeles, Houston, and Miami. The type of results shown in this table may provide some indications as to the usefulness of large-scale changes in surface albedo and vegetative fraction in various region. However, this preliminary modeling effort should be refined and expanded in the future to pave the way for more reliable conclusions.

4. Conclusion

This paper discussed results from a preliminary mesoscale modeling study to quantify the possible meteorological and energy-use impacts of large-scale increases in surface albedo and vegetative fraction in ten U.S. regions. Episodic seasonal mesoscale simulation results were interpolated to create a full year of hourly weather data for each region. Modified weather (mainly modified temperature) was used as input to a building energy model to assess the impacts of increased albedo and vegetative fraction on energy use.

The base-case mesoscale simulations suggest heat islands of 1–2 °C in most urban areas analyzed in this study. The simulations also suggest that large-scale increases in surface albedo and vegetative fraction can almost offset the urban heat island intensity in most of these areas. The energy implication of a 1–2 °C reduction in space-averaged air temperatures (around 2 pm local time) is a decrease of up to 10% in peak electricity demand. In terms of annual costs of energy use, the simulations suggest net savings in the order of $10–35 per 100 m^2 of roof area depending on building type and region. Areas like Los Angeles, Houston, Miami, and Phoenix seem to benefit most from

the large-scale surface modifications described in this paper, whereas regions like Philadelphia seem to benefit the least.

Appendix

Brief Model Description and Performance Evaluation

The CSUMM's formulation is based on the conservation laws, i.e., conservation of mass (continuity equation), potential temperature (heat), momentum, and water vapor:

$$\frac{\partial \rho}{\partial t} = -(\nabla \cdot \rho \mathbf{V}) \tag{A.1}$$

$$\frac{\partial \theta}{\partial t} = -\mathbf{V} \cdot \nabla\theta + S_\theta \tag{A.2}$$

$$\frac{\partial \mathbf{V}}{\partial t} = -\mathbf{V} \cdot \nabla\mathbf{V} - \frac{1}{\rho}\nabla p - g\mathbf{k} - 2\Omega \times \mathbf{V} \tag{A.3}$$

$$\frac{\partial q}{\partial t} = -\mathbf{V} \cdot \nabla q + S_q \tag{A.4}$$

where ρ is density, $\mathbf{V}$ is the wind velocity vector, θ is potential temperature, S_θ is sink/source term for potential temperature, p is pressure, g is gravitational acceleration, $\mathbf{k}$ is unit vector in the z-direction, Ω is angular velocity of the earth, q specific humidity, S_q is source/sink term for specific humidity.

The CSUMM is a hydrostatic, primitive-equation, three-dimensional Eulerian model originally developed by Pielke (1974). The model is incompressible, and employs a σ_Z coordinate system. It uses a first order closure scheme in treating sub-grid scale correlation terms of the governing differential equations. The model's domain in this application is 9-km high with an underlying soil layer 50-cm deep. The CSUMM generates three-dimensional fields of prognostic variables and a mixing height field.

Initially, Taha (1996) evaluated the CSUMM basecase model performance in simulating the Los Angeles Basin. In a separate effort, he also evaluated the performance of the model in simulating the Atlanta GA region. In the rest of this section, a very brief recap of the performance evaluation is given. For the Los Angeles basin, the observational data were obtained from the South Coast Air Quality Management District and, for the Atlanta region, they were obtained from the Georgia Automated Environmental Monitoring Network (GAEMN). GAEMN stations, maintenance, and related issues are discussed in Hoogenboom (1996).

The indices used in evaluating the base-case performance of the model include root mean square error (ε) of the simulation, unbiased root mean square error (ε') of the simulation, standard deviations of simulated and observed parameters (σ,σ_o), and the mean unsigned relative error (E) of the simulation. The latter is defined as:

$$E = \frac{1}{M}\Sigma|\mathbf{V}s_{ij} - \mathbf{V}o_{ij}|/\mathbf{V}o \tag{A.5}$$

Table 7. *Indices for Model Performance Evaluation*

JD	σ_o	σ	ε	ε'	ε'/σ_o	E
Los Angeles						
225 (cloudy)	3.7	4.6	5.2	4.2	1.13	18.3%
235 (clear)	6.2	4.6	4.9	4.4	0.70	17.2%
239 (cloudy)	4.5	4.6	7.1	3.2	0.71	32.5%
Atlanta						
208 (cloudy)	3.6	4.1	4.5	2.3	0.64	17.4%
211 (clear)	4.5	4.1	3.6	1.9	0.42	14.0%
214 (cloudy)	2.7	4.1	4.4	2.7	1.00	15.6%

where M is the number of available station-hours and Vs and Vo are respectively the simulated and observed values at station "i" and hour "j". The mean unsigned relative error criterion was devised for photochemical modeling but the concept is extended here for use in validating meteorological simulations. In this discussion, the parameter of interest is the air temperature at the lowest layer of the model.

Table 7 lists the values of these indices (for air temperature) computed based on episodic simulations of Los Angeles and Atlanta. According to Pielke (1984), Keyser and Anthes (1977), and EPA (1991), model skill is demonstrated if:

1) $\sigma \approx \sigma_o$,
2) $\varepsilon < \sigma_o$,
3) $\varepsilon' < \sigma_o$,
4) $\varepsilon'/\sigma_o \leq 0.6$, and
5) $E < 35\%$.

Thus we can see from Table 7 that the model's performance is acceptable on clear days (such as JD 235 in Los Angles and JD 211 in Atlanta) but not so during overcast ones. This is expected since the model does not include cloud or phase-change physics.

Acknowledgements

The author wish to thank Mr. Mark Decot, Project Manager at the U.S. DOE and Dr. Hashen Akbari, Leader of the Heat Island Project at the Lawrence Berkeley National Laboratory for their support and guidance. This work was sponsored by the United States Department of Energy under Contract No. DE-AC03-76SF00098.

References

Aida, M., 1982: Urban albedo as a function of the urban structure – A model experiment. *Bound. Layer Meteor.*, **23,** 405–413.

Akbari, H., Bretz, S., Taha, H., Kurn, D., Hanford, J., 1997a: Peak power and cooling energy savings of high-albedo roofs. *Energy and Buildings – Special Issue on Urban Heat Islands and Cool Communities,* pp. 117–126.

Akbari, H., Kurn, D., Bretz, S., Hanford, J., 1997b: Peak power and cooling energy savings of shade trees. *Energy and Buildings – Special Issue on Urban Heat Islands and Cool communities*, pp. 139–148.

Building Energy Simulation Group (BESG), 990: Overview of the DOE-2 Building Energy Analysis Program, Version 2.1D. Lawrence Berkeley Laboratory Report LBL-19735, Berkeley, CA, 1990.

Cassmassi, J. C., Durkee, K. R., 1990: Comparison of mixing height fields for UAM applications generated from limited and multiple temperature sounding profiles in the South Coast Air Basin. Technical paper presented at the A&WMA Tropospheric Ozone Conference, March 20–22 (1990), Industry Hills, CA.

EPA, 1991: Guideline for regulatory application of the Urban Airshed Model, EPA-450/4-91-013), Office of Air Quality Planning and Standards, Research Triangle Park, NC 27711.

Gabersek, S., Taha, H., 1996: Impacts of surface characteristics changes on urban heat island intensity. Proceedings of the ICB 96, 14th International Congress of Biometeorology, September 1–8, 1996, Ljubljana, Slovenija.

Hoogenboom, G., 1996: The Georgia Automated Environmental Monitoring Network. Proceedings of the 22nd Conference on Agricultural and Forest Meteorology, January 28-February 2, 1996, Atlanta, GA, pp. 343–346.

Horie, Y., Sidawi, S., Ellefsen, R., 1990: Inventory of leaf biomass and emission factors for vegetation in California's South Coast Air Basin. Final Report, Contract No. 90163, South Coast Air Quality Management District, Diamond Bar, California.

Kessler, R., Douglas, S., 1992: User's guide to the Systems Applications International Mesoscale Model. SYSAPP-92/069, Systems Applications International, San Rafael, California.

Keyser, D., Anthes, R.A., 1977: The application of a mixed-layer model of the planetary boundary layer to real data forecasting. *Mon. Wea. Rev.*, **105**, 1351–1371.

Konopacki, S.J., Akabari, H., Pomerantz, M., Gabersek, S., Gartland, L., 1997: Cooling Energy Savings Potential of Light-Colored Roofs for Residential and Commercial Buildings in 11 U.S. Metropolitan Areas. Lawrence Berkeley National Laboratory Report LBL-39433, Berkeley CA.

Linder, K.P., Inglis, M.R., 1989: The potential effects of climate change on regional and national demands for electricity, Chapter 1, pp. 1–38. In: The potential effects of climate global climate change on the United States. Appendix H, Report EPA-230-05-89-058, Environmental Protection Agency.

Liu, X., 1994: Estimating surface albedo using AVHRR satellite imagery, Chapter 3 In: Analysis of Energy Efficiency and Air Quality in the SoCAB – Phase II Pre-Final Report. LBL Report No. 35728, Berkeley, California.

Parker, D. S., Barkaszi, S. F., 1997: Roof solar reflectance and cooling energy use: Field research results from Florida. *Energy and Buildings – Special Issue on Urban Heat Islands and Cool Communities*, pp. 99–104.

Pielke, R., 1984: *Mesoscale Meteorological Modeling.* Academic press, 612 pp.

Pielke, R., 1974: A three-dimensional numerical model of the sea breeze over South Florida. *Mon. Wea. Rev.*, **102**, 115–139.

Sailor, D., 1993: Role of surface characteristics in urban meteorology and air quality. Lawrence Berkeley National Laboratory Report No. 34459, UC-Berkeley, Doctoral Thesis.

Sievers, U., Zdunkowski, W., 1985: A numerical simulation scheme for the albedo of city street canyons. *Bound. Layer Meteor.*, **33**, 245–257.

Simpson, J. R., McPherson, E. G., 1997: The effects of roof albedo modification on residential cooling loads in Tucson, Arizona. *Energy and Buildings – Special Issue on Urban Heat Islands and Cool Communities*, pp. 127–138.

Taha, H., 1996: Modeling the impacts of increased urban vegetation on the ozone air quality in the south coast air basin. *Atmos. Environ.*, **30** 20, 3423–3430.

Taha, H., 1997: Modeling the impacts of large-scale albedo changes on ozone air quality in the south coast air basin. *Atmos. Environ.*, **31** 11, 1667–1676.

Taha, H., Akbari, H., Rosenfeld, A., 1988: Residential Cooling Loads and the Urban Heat Island: The Effects of Albedo. *Building and Environment*, **23** 4, 271–283.

Vihma, T., Savijarvi, H., 1991: On the effective roughness length for heterogeneous terrain. *Quart. J. Roy. Meteor. Soc.*, **117**, 399–407.

Authors' address: Dr. Haider Taha, Staff Scientist, MS 90-2000, Lawrence Berkeley National Laboratory, Berkeley, California 94720, U.S.A.; Steven Konopacki and Sasa Gabersek, Heat Island Project, Environmental Energy Technologies division, Lawrence Berkeley National Laboratory, Berkeley, California 94720, U.S.A.